NAMRC 53

THE UNIVERSITY OF TENNESSEE KNOXVILLE

A Cutting Mechanics-based Machine Learning Modeling Method to Discover Governing Equations of Machining Dynamics

Mason Ma

Joint work with Alisa Ren, Jiajie Wu, Jaydeep Karandikar, Chris Tyler, Tony Shi and Tony Schmitz

Manufacturing Mind&Physics Laboratory (MINDS Lab)
Machine Tool Research Center (MTRC)
University of Tennessee Knoxville

hma19@vols.utk.edu

June 24, 2025

Outline

1. Introduction
2. Proposed Cutting Mechanics-based Machine Learning (CMML)
3. Simulation Experiments
4. Conclusion

Introduction

Introduction to Machine Tool Chatter

- **Machining Dynamics** studies the physical process of metal cutting to describe the tool-workpiece engagement
  - Machine tool structural dynamics
  - Cutting forces

- **Machine Tool Chatter**: self-excited vibrations of the machine tool, fundamental physical phenomenon in machining
  - Limits material removal rate, productivity, surface quality, and geometric accuracy of machined parts.

Milling machine tool

Machining process

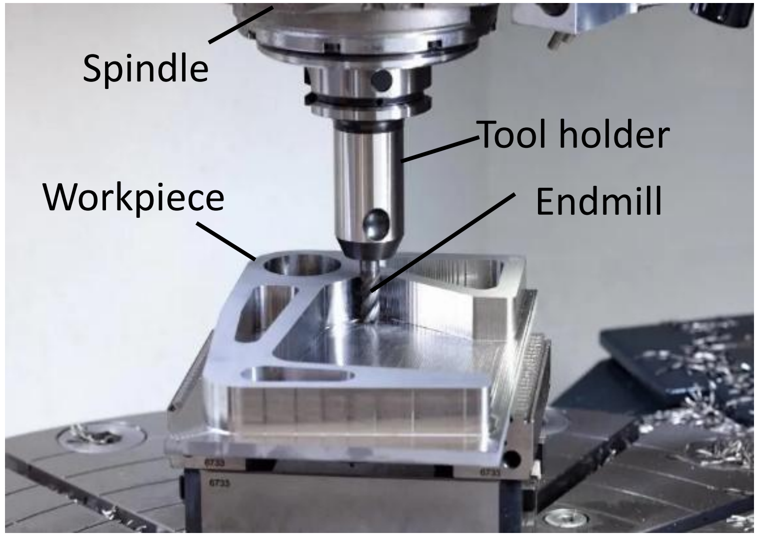

Machined parts

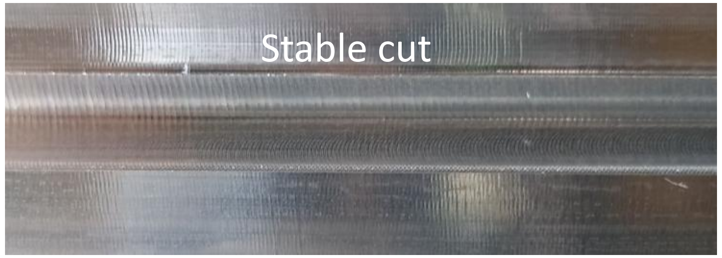

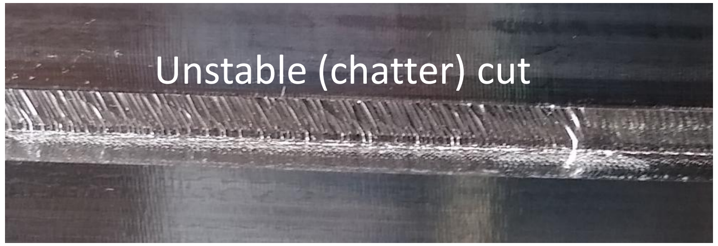

Image source: CNCLathing.com

Modeling of Tool-Workpiece Engagement

Machine tool chatter can be mathematically described by the **second order, coupled, time delay differential equations (DDE)** of motion:

$$\underbrace{[\boldsymbol{m}]\ddot{\boldsymbol{x}}(t) + [\boldsymbol{c}]\dot{\boldsymbol{x}}(t) + [\boldsymbol{k}]\boldsymbol{x}(t)}_{\text{Structural dynamics}} = \underbrace{\boldsymbol{F}(\boldsymbol{K}, \boldsymbol{x}(t) - \boldsymbol{x}(t-\tau), \dot{\boldsymbol{x}}, \boldsymbol{u})}_{\text{Cutting force model}},$$

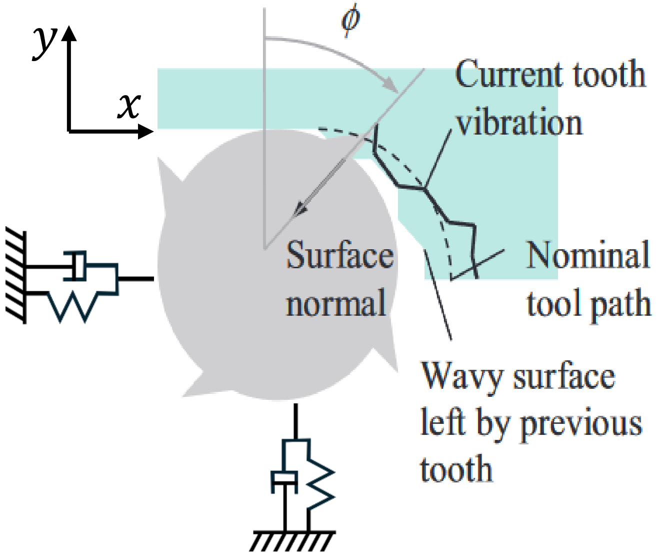

- $\ddot{\boldsymbol{x}}(t), \dot{\boldsymbol{x}}(t), \boldsymbol{x}(t)$: Tool/workpiece acceleration, velocity, and displacement
- $[\boldsymbol{m}], [\boldsymbol{c}], [\boldsymbol{k}]$: Modal mass, viscous damping, and stiffness matrices
- $\boldsymbol{F}(\cdot)$: instantaneous dynamic cutting force model

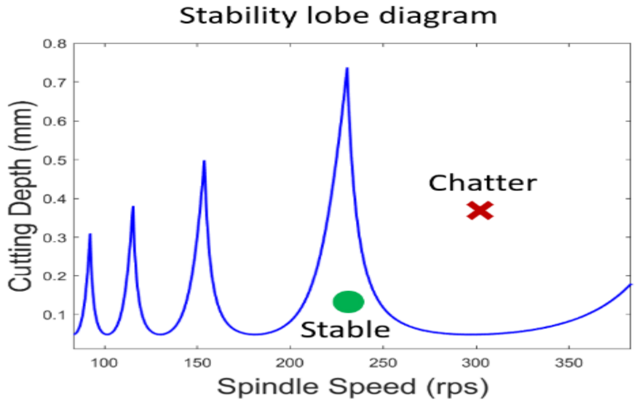

Linear force models for $\boldsymbol{F}(\cdot)$ are dominant.

Overview of Modeling Efforts

- **Linear models: very mature; to fully utilize existing linear stability theory**
  - First machining dynamics model (turning): Non-autonomous (time invariant) nonlinear DDE (Doi and Kato, 1956)
  - Pioneer work: in-contact cutting to establish linear chatter theory (Tobias and Fishwick, 1958; Tlusty and Polacek, 1963)
  - First machining dynamics model (milling): Autonomous (time variant) linear DDEs (Sridhar et al., 1968)
  - Models considering process damping, edge force, and runout (Sweeney and Tobias 1969; Schmitz et al., 2007; Tyler and Schmitz, 2013)
  - Modeling for better structural dynamics prediction: Receptance coupling substructure analysis (Schmitz and Donalson, 2000)
- **Nonlinear models: seldomly explored; difficult for stability map generation**
  - Time domain simulation (Tlusty and Ismail, 1981; Smith and Tlusty, 1991; Smith and Tlusty, 1993; Wiecigroch and Budak, 2001)
    - Complicated tool geometries (e.g., runout, different radii, non-uniform teeth spacing, variable helix angles, etc.)
    - Nonlinearity that occurs due to interrupted cutting caused by loss-of-contact.
  - Nonlinear dynamics and chaos (Hanna and Tobias 1974; Shi and Tobias, 1984; Moon and Kalmar-Nagy, 2001)
  - Data-driven methods – Machine learning (ML) models:
    - Accurate coefficient estimation for existing models (Vaishnav and Desai, 2022; Rubeo and Schmitz, 2016; Kim et al., 2025)
    - Accurate stability solution (neural network (Cherukuri et al., 2019); support vector machine (Greis et al., 2023); k-nearest neighbors (Schmitz, 2024); physics-based Bayesian learning (Karandikar et al., 2020; Schmitz et al., 2022))

Research question:

How to obtain an accurate nonlinear cutting force model to better describe the tool-workpiece engagement?

Proposed Cutting Mechanics-based Machine Learning (CMML) Modeling Method

Idea of CMML

Basic Idea of the proposed cutting mechanics-based machine modeling method (CMML):

- Integrate existing physics knowledge of cutting mechanics and unknown physics in data, to automatically discover the governing equations of machining dynamics

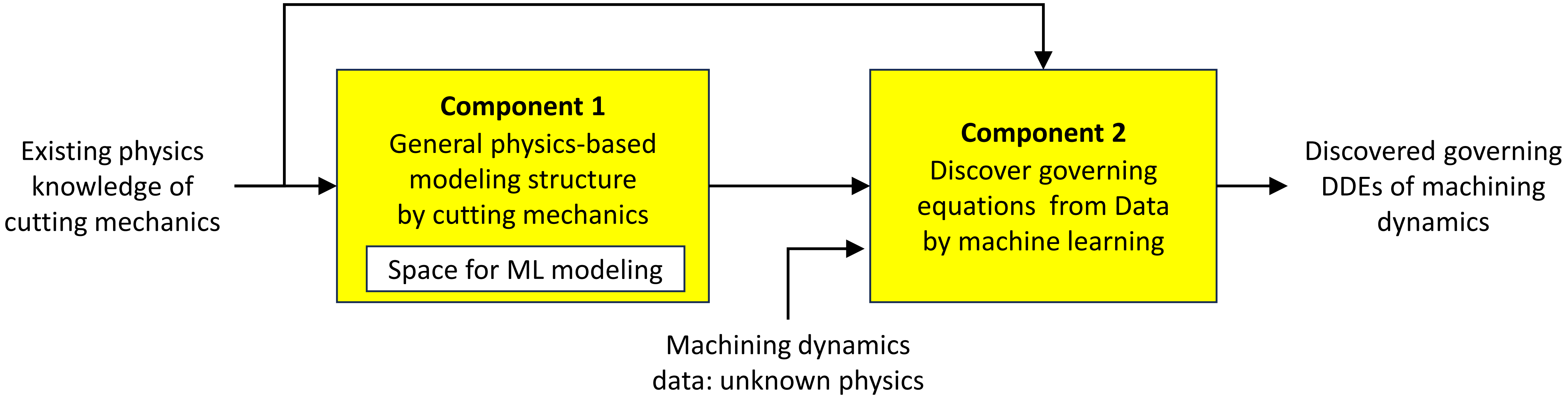

- Feasibility study with potential to advance machining modeling using experimental data.

Component I:

Establish Physics-based Modeling Structure by Cutting Mechanics

Two Fundamental Principles of Cutting Mechanics

1. Time Delay

The wavy surface of previous cut is modulated into the current wavy surface, generating the time delay term $n(t-\tau)-n(t)$. This generates dynamic cutting forces and chatter. **Instantaneous chip thickness** is determined by time-delay effect as

$$h(t) = f_t \sin(\phi) + \boxed{n(t-\tau)-n(t)}$$

Dynamic chip thickness caused by time delay effect

2. Cutting Force Projection

- Resultant dynamic cutting forces are exerted on tangential and normal directions. F_n and F_t can be expressed as:

$$F_t(t) = f_t(n(t-\tau)-n(t), \dot{n}(t), \boldsymbol{u}),$$

$$F_n(t) = f_n(n(t-\tau)-n(t), \dot{n}(t), \boldsymbol{u}).$$

- The projection relationship to project F_t and F_n onto machine tool's coordinate, x and y directions will be

$$\boxed{\begin{aligned} F_x &= -F_t \cos(\phi) + F_n \sin(\phi), \\ F_y &= F_t \sin(\phi) + F_n \cos(\phi). \end{aligned}}$$

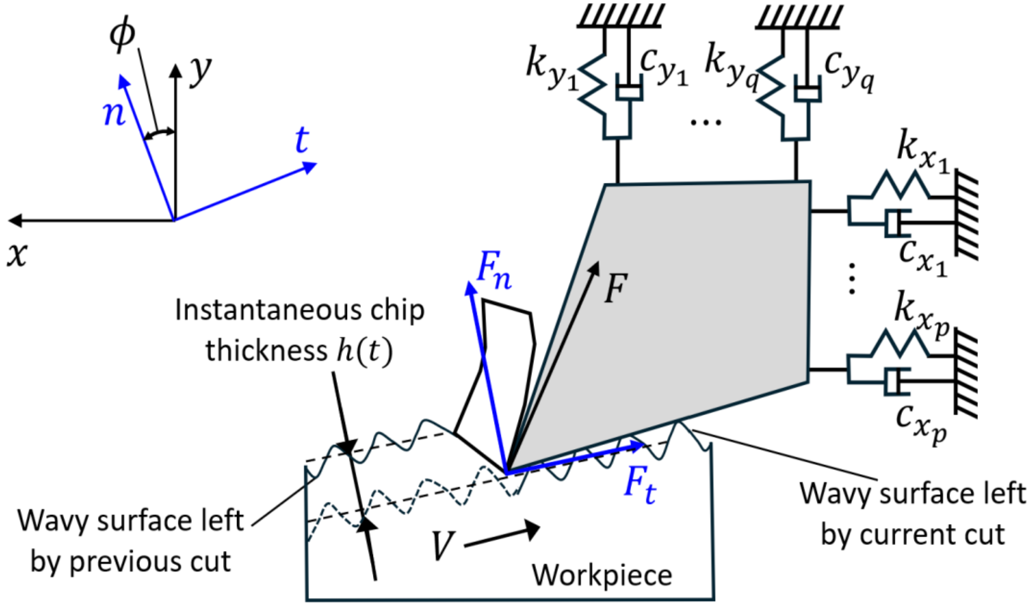

General Cutting Mechanics-based Modeling Structure

- Original DDEs is written in canonical form:

$$[\boldsymbol{m}_x]\ddot{\boldsymbol{x}} + [\boldsymbol{c}_x]\dot{\boldsymbol{x}} + [\boldsymbol{k}_x]\boldsymbol{x} = \boldsymbol{F}_x(t, \boldsymbol{x}(t), \boldsymbol{x}(t-\tau), \dot{\boldsymbol{x}}),$$
$$[\boldsymbol{m}_y]\ddot{\boldsymbol{y}} + [\boldsymbol{c}_y]\dot{y} + [\boldsymbol{k}_y]\boldsymbol{y} = \boldsymbol{F}_y(t, \boldsymbol{y}(t), \boldsymbol{y}(t-\tau), \dot{\boldsymbol{y}})$$

- Reformulate DDEs into a set of **differential algebraic equations (DAEs):**
  - **Differential equations (DEs)** for state variables: let $\boldsymbol{s}(t) = [\boldsymbol{x}(t), \boldsymbol{v}_x(t), \boldsymbol{y}(t), \boldsymbol{v}_y(t)]$

Structural dynamics

$$\boxed{\begin{aligned} \dot{\boldsymbol{x}} &= \boldsymbol{f}_1(\boldsymbol{s}(t), \boldsymbol{u}, \boldsymbol{F}(t)), && (1) \\ \dot{\boldsymbol{v}}_x &= \boldsymbol{f}_2(\boldsymbol{s}(t), \boldsymbol{u}, \boldsymbol{F}(t)), && (2) \\ \dot{\boldsymbol{y}} &= \boldsymbol{f}_3(\boldsymbol{s}(t), \boldsymbol{u}, \boldsymbol{F}(t)), && (3) \\ \dot{\boldsymbol{v}}_y &= \boldsymbol{f}_4(\boldsymbol{s}(t), \boldsymbol{u}, \boldsymbol{F}(t)). && (4) \end{aligned}}$$

DAEs (1) – (6) are unknown and will be discovered using discrete optimization-based machine learning method.

  - **Algebraic equations (AEs)** for cutting forces

Cutting force models

$$\boxed{\begin{aligned} F_n &= g_1(\boldsymbol{x}(t), \boldsymbol{x}(t-\tau), \boldsymbol{y}(t), \boldsymbol{y}(t-\tau), \boldsymbol{u}), \\ F_t &= g_2(\boldsymbol{x}(t), \boldsymbol{x}(t-\tau), \boldsymbol{y}(t), \boldsymbol{y}(t-\tau), \boldsymbol{u}), \end{aligned}}$$

$$\boxed{\begin{aligned} F_x &= -F_t(t)\cos(\phi) + F_n(t)\sin(\phi), \\ F_y &= F_t(t)\sin(\phi) + F_n(t)\cos(\phi). \end{aligned}}$$

Clearly known projection relationship

Component II:

Discover Differential Algebraic Equations from Data by Machine Learning

Discover DAEs from Data by Machine Learning

- **Measurable data by assumption**
  - $\mathbf{S} \in \mathbb{R}^{N\times(2p+2q)}$: time series data of state variables $\boldsymbol{s}(t) = [\boldsymbol{x}(t), \boldsymbol{v}_x(t), \boldsymbol{y}(t), \boldsymbol{v}_y(t)]$
  - $\dot{\mathbf{S}} \in \mathbb{R}^{N\times(2p+2q)}$: time series data of time derivatives of state variables $\dot{\boldsymbol{s}}(t)$.
    - $\dot{\mathbf{S}}$ can be numerically calculated from $\mathbf{S}$
  - $\mathbf{F} \in \mathbb{R}^{N\times 2}$: time series data of cutting forces
  - $\mathbf{U} \in \mathbb{R}^{N\times r}$: data matrix of process parameters as paired data of $\mathbf{S}$, $\dot{\mathbf{S}}$, and $\mathbf{F}$
  - Reasonable assumption: the dynamometers, capacitance probes, laser vibrometers, and accelerometers were used to concurrently measure cutting force, displacement, velocity and acceleration
  - Data is subjected to noises

- The ML algorithm is developed by customizing the discrete-optimization based ML method for discovering differential equations of nonlinear dynamics in [1]
- It is general to all unknown DAES, without loss of generality, j-th differential equation for x displacement will be discovered

$$\dot{x}_j = f_j(\boldsymbol{s}, \boldsymbol{u}, \boldsymbol{F})$$

[1] Shi, T., Ma, M., Tran, H. and Zhang, G., 2025. Compressive-Sensing-Assisted Mixed Integer Optimization for Dynamical System Discovery With Highly Noisy Data. Numer. Methods Partial Differ. Equ., 41(1), p.e23164.

Cutting Mechanics-based Nonlinear Learning Function Space Design

1. **Cutting mechanics-based candidate physical terms design:**
   - A cutting mechanics-based candidate set consisting of a total of ***P* candidate physical terms** for $f(\boldsymbol{s}, \boldsymbol{u}, \boldsymbol{F})$

     $$\boldsymbol{\theta}(\boldsymbol{s}, \boldsymbol{u}, \boldsymbol{F}) \coloneqq [\theta_1(\boldsymbol{s}, \boldsymbol{u}, \boldsymbol{F})\ \theta_2(\boldsymbol{s}, \boldsymbol{u}, \boldsymbol{F}) \cdots \theta_P(\boldsymbol{s}, \boldsymbol{u}, \boldsymbol{F})],$$

   - Integrating existing knowledge of cutting mechanics:

     $$\boldsymbol{\theta}(\boldsymbol{s}, \boldsymbol{u}, \boldsymbol{F}) = [1\ \boldsymbol{s}\ \boldsymbol{u}\ \boldsymbol{F}\ \boldsymbol{s}^2\ \boldsymbol{s} \otimes \boldsymbol{u}\ \boxed{n(t-\tau) - n(t)}\ \sin\phi \ldots].$$

     Embed time delay term in the candidate set directly

2. **Learning function space construction:**
   - ***Assumption 1:*** all functions $f(\boldsymbol{s}, \boldsymbol{u}, \boldsymbol{F})$ live in the affine functional space expanded by $\boldsymbol{\theta}(\boldsymbol{s}, \boldsymbol{u}, \boldsymbol{F})$.

     $$f(\boldsymbol{s}, \boldsymbol{u}, \boldsymbol{F}) = \boldsymbol{\theta}(\boldsymbol{s}, \boldsymbol{u}, \boldsymbol{F}) \cdot \boxed{\boldsymbol{\xi},}$$

     $\boldsymbol{\xi} = [\xi_1\ \ \xi_2\ \ \cdots\ \ \xi_P]^T \in \mathbb{R}^{P\times 1}$ denotes the vector of coefficients of each physical term

   - ***Assumption 2:*** The physical terms in RHS of above equation are sparse in predefined function space. Namely, the number of active terms in $f(\boldsymbol{s}, \boldsymbol{u}, \boldsymbol{F})$ is much smaller than that in the candidate set $\boldsymbol{\theta}(\boldsymbol{s}, \boldsymbol{u}, \boldsymbol{F})$.

Discover DAEs by Discrete Optimization-based Learning Algorithm

- Introduce a new binary variable $\boldsymbol{\gamma} = [\gamma_1\ \gamma_2\ \dots \gamma_P]^T \in \mathbb{B}^{P\times 1}$ to indicate the presence of physical term θ_p in $f(\boldsymbol{s}, \boldsymbol{u}, \boldsymbol{F})$.

$$\gamma_p = \begin{cases} 1, & \text{if } f(\boldsymbol{s}, \boldsymbol{u}, \boldsymbol{F}) \text{ includes } \theta_p \\ 0, & \text{otherwise} \end{cases}, \qquad \forall p \in [P],$$

- A sparse linear regression model can be constructed as

l_0-norm constraints the number of nonzero entries of ξ

$$\min_{\boldsymbol{\gamma},\boldsymbol{\xi}} \|\dot{\boldsymbol{x}} - \boldsymbol{\Theta}(\mathbf{S}, \mathbf{U}, \mathbf{F}) \cdot (\boldsymbol{\gamma} \circ \boldsymbol{\xi})\|_2^2 + \underline{\lambda_0 \|\boldsymbol{\xi}\|_0} + \underline{\lambda_2 \|\boldsymbol{\xi}\|_2^2}.$$

l_2-norm reduces effect of noise

  - reformulation:

$$\min_{\boldsymbol{\gamma},\boldsymbol{\xi}} \boxed{\|\dot{\boldsymbol{x}} - \boldsymbol{\Theta}(\mathbf{S}, \mathbf{U}, \mathbf{F}) \cdot \boldsymbol{\xi}\|_2^2} + \lambda_2 \|\boldsymbol{\xi}\|_2^2$$

Sum of squared errors between measurements $\dot{x}$ and model prediction

$$s.t.\ -M\boldsymbol{\gamma} \le \boldsymbol{\xi} \le M\boldsymbol{\gamma},$$

Element-wise relationship. When $\gamma_p = 0, \xi_p = 0$. When $\gamma_p = 1, \xi_p$ is bounded by $[-M, M]$.

$$\langle \boldsymbol{\gamma}, \boldsymbol{e} \rangle = k,$$

The number of active physical terms.

$$\boldsymbol{\gamma} \in \mathbb{B}^{P\times 1}, \boldsymbol{\xi} \in \mathbb{R}^{P\times 1}.$$

- Once solved, $\boldsymbol{\gamma}^*$ and $\boldsymbol{\xi}^*$ are obtained, the governing equation is

$$\dot{x} = \boldsymbol{\theta}(\boldsymbol{s}, \boldsymbol{u}, \boldsymbol{F}) \cdot (\boldsymbol{\gamma}^* \circ \boldsymbol{\xi}^*).$$

Simulation Experiments

Simulation Experiment Settings

Two case studies of governing equations discovery for milling dynamics:

- Case I: Milling dynamics with only time delayed effect in the cutting force model
- Case II: Milling dynamics with time delayed effect, process damping, and edge force in the force model

Data generation:

- Time series data is generated by experimentally verified time domain simulation
- Gaussian noise is added to each measurable variable, $\boldsymbol{S}^{noise} = \boldsymbol{S} + r\sigma_S\boldsymbol{\epsilon}$, where $r = \{0, 0.01\%, 0.1\%, 1\%, 10\%, 50\%, 100\%\}$

Parameter setting of proposed CMML

- The number of active terms k is set to be exact number of physical terms in milling dynamics model
- l_2-norm weight, $\lambda_2 = 100$
- $M = 1000$
- The discrete optimization solver: CPLEX 20.1.0.

Performance metric

- Number of exactly discovered DAEs:

$$A := \sum_{i=1}^{2p+2q+2} 1_{\gamma_i^* = \gamma_i^\dagger} = \begin{cases} 1, & \text{if } \gamma_i^* = \gamma_i^\dagger \\ 0, & \text{if } \gamma_i^* \neq \gamma_i^\dagger \end{cases}.$$

Measure the accuracy of term identification: $A = 2p + 2q + 2$, fully discovered all DAEs

- Accuracy of coefficients of discovered governing equations: Mean Absolute Percentage Error (MAPE)

$$MAPE := \frac{1}{\sum_{i=1}^{2p+2q+2} \left\|\boldsymbol{\gamma}_i^\dagger\right\|_0} \sum_{i=1}^{2p+2q+2} \sum_{p=1}^{\left\|\boldsymbol{\gamma}_i^\dagger\right\|_0} \left| \frac{\xi_{ip}^* - \xi_{ip}^\dagger}{\xi_{ip}^\dagger} \right| \times 100\%.$$

Measure the accuracy of coefficient estimation (the smaller the better)

Case I: Milling with Only Time Delayed Effect in forces

The equations of motion for machining dynamics

$$m_x\ddot{x}(t) + c_x\dot{x}(t) + k_x x(t) = F_x(t),$$
$$m_y\ddot{y}(t) + c_y\dot{y}(t) + k_y y(t) = F_y(t).$$

The cutting forces on x and y directions:

$$F_x = -F_t\cos(\phi) + F_n\sin(\phi)\,,$$
$$F_y = F_t\sin(\phi) + F_n\cos(\phi)\,.$$

The tangential and normal force models:

$$F_t(t) = k_t b\big(f_t\sin\phi + n(t-\tau) - n(t)\big),$$
$$F_n(t) = k_n b\big(f_t\sin\phi + n(t-\tau) - n(t)\big).$$

The Ground Truth DAEs for the Studied Milling System:

$$\boxed{\begin{aligned}
\dot{x} &= v_x,\\
\dot{v}_x &= \frac{-c_x v_x - k_x x + F_x}{m_x},\\
\dot{y} &= v_y,\\
\dot{v}_y &= \frac{-c_y v_y - k_y y + F_y}{m_y},\\
F_t &= k_{tc}b\big(f_t\sin\phi + n(t-\tau) - n(t)\big),\\
F_n &= k_{nc}b\big(f_t\sin\phi + n(t-\tau) - n(t)\big),
\end{aligned}}$$
$$\begin{aligned}
F_x &= -F_t\cos(\phi) + F_n\sin(\phi)\,,\\
F_y &= F_t\sin(\phi) + F_n\cos(\phi)\,.
\end{aligned}$$

Linear model

Case I: Milling with time delayed effect in forces

Accuracy of CMML for discovering governing equations

Table 1: Number of correct DAEs (A value) discovered by CMML for the milling dynamics in Case I (with only time delayed effect in force models).

	Spindle Speed Ω (rpm)				
Noise ratio r (%)	4000	6000	8000	10000	12000
Noise Free	**6**	**6**	**6**	**6**	**6**
0.01%	**6**	**6**	**6**	**6**	**6**
0.1%	**6**	**6**	**6**	**6**	**6**
1%	**6**	**6**	**6**	**6**	**6**
10%	**6**	**6**	**6**	**6**	**6**
50%	5	**6**	5	4	4
100%	4	4	4	4	4
500%	4	4	3	4	3
1000%	2	2	2	2	2

Noise ratio r	0.01%	0.1%	1%	10%	50%
MAPE	0.00%	0.00%	0.01%	0.33%	7.92%

Table 2: Discovered DAEs for the milling dynamics in Case I (with only time delayed effect in force model for Ω = 6000 rpm in Table 1).

Noise ratio r (%)	Discovered DAEs
Noise Free (exact governing equations)	$\dot{x} = v_x$ $\dot{v}_x = -25266187.27x - 100.53v_x + 5.05F_x$ $\dot{y} = v_y$ $\dot{v}_y = -25266187.27y - 100.53v_y + 5.05F_y$ $F_t = -695387890.93\Delta nb + 69538.79 \sin\phi\, b$ $F_n = 280954945.06\Delta nb - 28095.50 \sin\phi\, b$
0.01%	$\dot{x} = v_x$ $\dot{v}_x = -25266192.30x - 100.53v_x + 5.05F_x$ $\dot{y} = v_y$ $\dot{v}_y = -25266191.61y - 100.53v_y + 5.05F_y$ $F_t = -695387669.36\Delta nb + 69538.81 \sin\phi\, b$ $F_n = 280954790.02\Delta nb - 28095.48 \sin\phi\, b$
0.1%	$\dot{x} = v_x$ $\dot{v}_x = -25266237.52x - 100.53v_x + 5.05F_x$ $\dot{y} = v_y$ $\dot{v}_y = -25266230.73y - 100.53v_y + 5.05F_y$ $F_t = -695385675.23\Delta nb + 69539.00 \sin\phi\, b$ $F_n = 280953394.63\Delta nb - 28095.36 \sin\phi\, b$
1%	$\dot{x} = v_x$ $\dot{v}_x = 25266679.36x - 100.55v_x + 5.05F_x$ $\dot{y} = v_y$ $\dot{v}_y = -25266620.77y - 100.50v_y + 5.05F_y$ $F_t = -695365734.00\Delta nb + 69540.87 \sin\phi\, b$ $F_n = 280939440.76\Delta nb - 28094.17 \sin\phi\, b$
10%	$\dot{x} = v_x$ $\dot{v}_x = -25270056.27x - 99.72v_x + 5.04F_x$ $\dot{y} = v_y$ $\dot{v}_y = -25270392.27y - 98.84v_y + 5.03F_y$ $F_t = -695166321.72\Delta nb + 69559.61 \sin\phi\, b$ $F_n = 280799902.02\Delta nb - 28082.23 \sin\phi\, b$
50%	$\dot{x} = v_x$ $\dot{v}_x = -25262721.75x - 75.51v_x + 4.70F_x$ $\dot{y} = v_y$ $\dot{v}_y = -25282589.36y - 66.14v_y + 4.43F_y$ $F_t = -694280044.90\Delta nb + 69642.87 \sin\phi\, b$ $F_n = 280179729.87\Delta nb - 28029.19 \sin\phi\, b$

Number of discovered equations: A

CMML can discover from noisy data with the noise ratio up to 50%.

Accuracy of the coefficients: MAPE

The deviation of CMML estimated coefficients is almost 0% for low noise levels and at most 7.92%.

Computation time of CMML is **7.76 seconds** on average for discovering DAEs

Simulation Experiment – Case I

Case I: Milling with time delayed effect in forces

Stability lobes diagrams of discovered governing equations

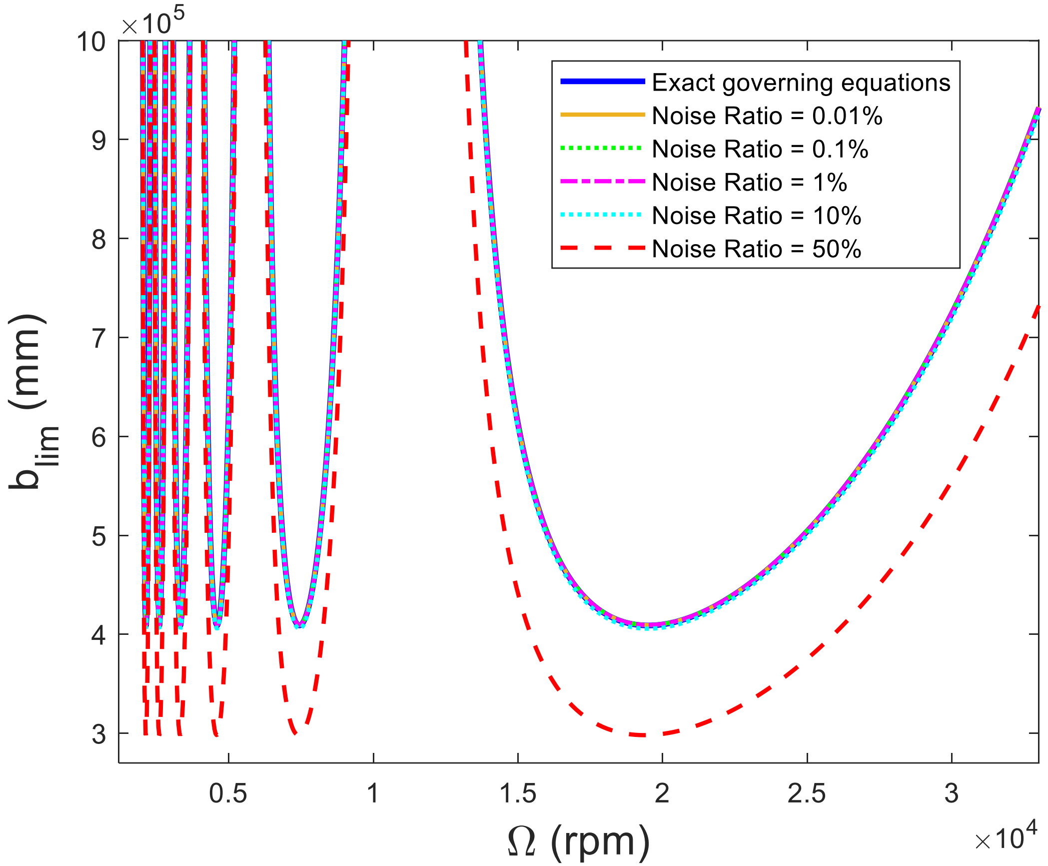

The stability lobe diagrams for $\Omega = 6000$ rpm in Table 2

- Model discovered by CMML is analytical model → directly used as input in stability solution method (Zero-order approximation) to generate stability lobe diagram.
- Use discovered DAEs with noise ratio from 0.00% (exact governing equations) to 50% to generate SLD.
- Except noise ratio = 50%, all other results almost overlap with lobes by exact governing equations.

Simulation Experiment – Case I

Case I: Milling with time delayed effect in forces

Time series trajectories and phase plane plots

- The single group of rad points indicates that sampled points repeat, and the milling operation is stable.
- Two results of exact governing equations and DAEs discovered by CMML show the good agreement with each other.

Simulation of discovered governing equations match well with the ground truth → high accuracy of CMML discovered DAEs

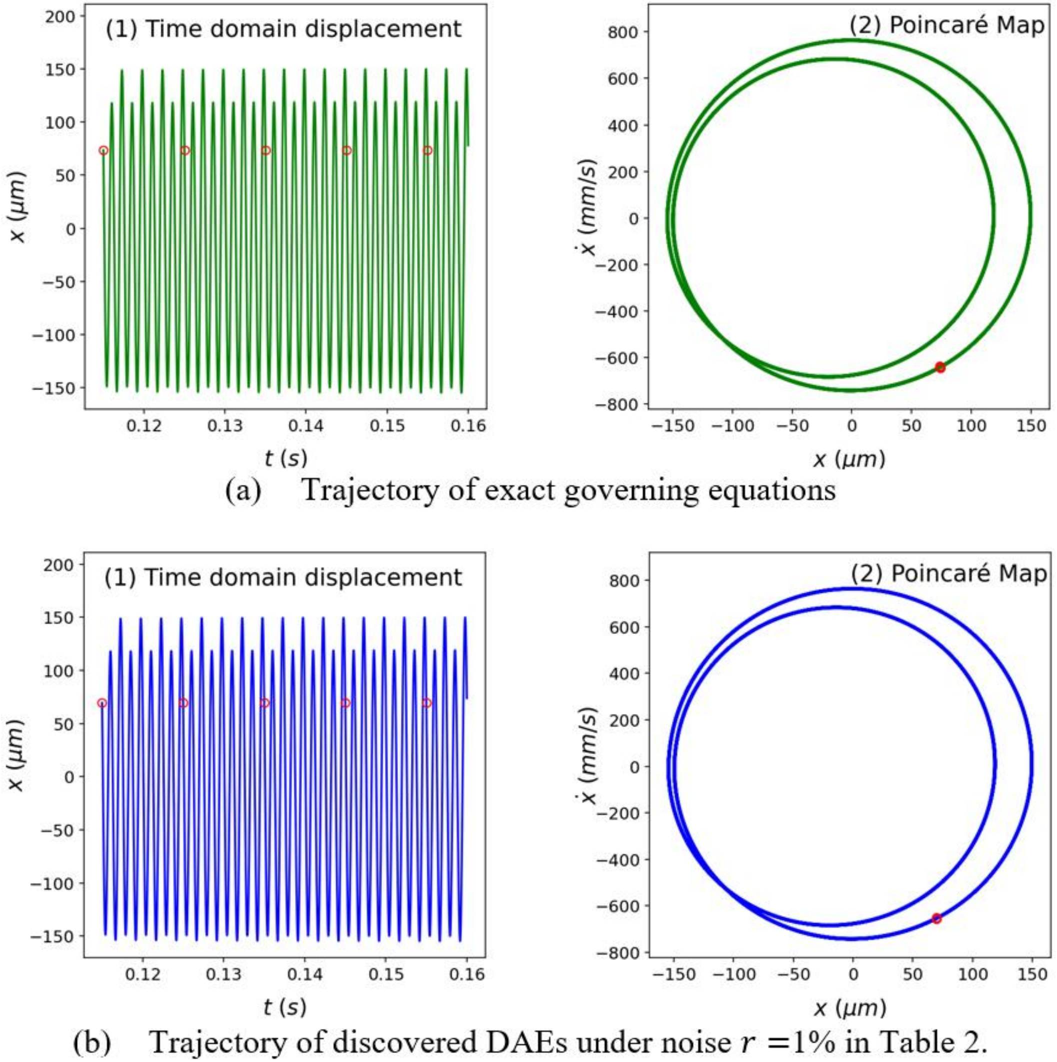

Time domain displacement (on x direction) and Poincaré map of discovered equations in Table 2 using parameters Ω=6000 rpm and b= 2 mm.

Simulation Experiment – Case II

Case II: Milling with time delayed effect, **process damping** and **edge force**

The Ground Truth DAEs for the Studied Milling Dynamics with NONLINEAR Term

$$\dot{x} = v_x,$$

$$\dot{v}_x = \frac{-c_x v_x - k_x x + F_x}{m_x},$$

$$\dot{y} = v_y,$$

$$\dot{v}_y = \frac{-c_y v_y - k_y y + F_y}{m_y},$$

$$F_t = k_{tc} b\big(f_t \sin\phi + n(t-\tau) - n(t)\big) + \boxed{k_{te} b} + \boxed{C_t \frac{b}{V}\dot{n}^2},$$

$$F_n = k_{nc} b\big(f_t \sin\phi + n(t-\tau) - n(t)\big) + \boxed{k_{ne} b} + \boxed{C_n \frac{b}{V}\dot{n}^2}.$$

$$F_x = -F_t \cos(\phi) + F_n \sin(\phi),$$

$$F_y = F_t \sin(\phi) + F_n \cos(\phi).$$

Process damping term: informally introduced

Edge force

Nonlinear

Case I: Milling with time delayed, process damping, and edge force

Accuracy of CMML for discovering governing equations

Table 3: Number of correct DAEs (A value) discovered by CMML for the milling dynamics in Case II with time delayed effect, nonlinear process damping, and edge effect in the force models.

	Spindle Speed Ω (rpm)				
Noise ratio r (%)	4000	6000	8000	10000	12000
Noise Free	**6**	**6**	**6**	**6**	**6**
0.01%	**6**	**6**	**6**	**6**	**6**
0.1%	**6**	**6**	**6**	**6**	**6**
1%	**6**	**6**	**6**	**6**	**6**
10%	**6**	**6**	4	5	**6**
50%	**6**	**6**	2	2	4
100%	4	4	3	3	3
500%	2	3	2	2	2
1000%	2	2	2	2	2

Noise ratio r	0.01%	0.1%	1%	10%	50%
MAPE	0.00%	0.00%	0.05%	0.68%	8.03%

Table 4: Discovered DAEs for the milling dynamics in Case II (with time delayed effect, nonlinear process damping, and edge effect in the force models for Ω = 6000 rpm in Table 3).

Noise ratio r (%)	Discovered DAEs
Noise Free (exact governing equations)	$\dot{x} = v_x$ $\dot{v}_x = -25266187.27x - 100.53v_x + 5.05F_x$ $\dot{y} = v_y$ $\dot{v}_y = -25266187.27y - 100.53v_y + 5.05F_y$ $F_t = 25000.00b - 695387890.92\Delta nb + 69538.79 \sin\phi\, b - 222.82\dot{n}^2 b$ $F_n = 25000.00b + 280954945.06\Delta nb - 28095.49 \sin\phi\, b + 222.82\dot{n}^2 b$
0.01%	$\dot{x} = v_x$ $\dot{v}_x = -25266185.24x - 100.53v_x + 5.05F_x$ $\dot{y} = v_y$ $\dot{v}_y = -25266192.35y - 100.53v_y + 5.05F_y$ $F_t = 25000.44b - 695388128.39\Delta nb + 69538.33 \sin\phi\, b - 222.81\dot{n}^2 b$ $F_n = 24999.86b + 280954746.63\Delta nb - 28095.88 \sin\phi\, b + 222.82\dot{n}^2 b$
0.1%	$\dot{x} = v_x$ $\dot{v}_x = -25266166.88x - 100.54v_x + 5.05F_x$ $\dot{y} = v_y$ $\dot{v}_y = -25266237.93y - 100.53v_y + 5.05F_y$ $F_t = 25004.41b - 695390265.56\Delta nb + 69534.22 \sin\phi\, b - 222.80\dot{n}^2 b$ $F_n = 24998.61b + 280952960.82\Delta nb - 28099.37 \sin\phi\, b + 222.83\dot{n}^2 b$
1%	$\dot{x} = v_x$ $\dot{v}_x = -25265972.09x - 100.59v_x + 5.05F_x$ $\dot{y} = v_y$ $\dot{v}_y = -25266678.29y - 100.46v_y + 5.05F_y$ $F_t = 25044.14b - 695411637.29\Delta nb + 69493.07 \sin\phi\, b - 222.61\dot{n}^2 b$ $F_n = 24986.10b + 280935102.62\Delta nb - 28134.27 \sin\phi\, b + 222.96\dot{n}^2 b$
10%	$\dot{x} = v_x$ $\dot{v}_x = -25262914.86x - 99.77v_x + 5.04F_x$ $\dot{y} = v_y$ $\dot{v}_y = -25269532.49y - 98.42v_y + 5.03F_y$ $F_t = 25441.38b - 695625354.64\Delta nb + 69081.56 \sin\phi\, b - 220.80\dot{n}^2 b$ $F_n = 24861.03b + 280756520.68\Delta nb - 28483.26 \sin\phi\, b + 224.26\dot{n}^2 b$
50%	$\dot{x} = v_x$ $\dot{v}_x = -25227362.02x - 69.90v_x + 4.73F_x$ $\dot{y} = v_y$ $\dot{v}_y = -25249866.63y - 62.19v_y + 4.69F_y$ $F_t = 27206.92b - 696575209.50\Delta nb + 67252.64 \sin\phi\, b - 212.71\dot{n}^2 b$ $F_n = 24305.18b + 279962823.18\Delta nb - 30034.33 \sin\phi\, b + 230.01\dot{n}^2 b$

Number of discovered equations: A

CMML can discover from noisy data with the noise ratio up to 50%.

Accuracy of the coefficients: MAPE

The deviation of CMML estimated coefficients is almost 0% for low noise levels and at most 8.03%.

Computation time of CMML is **9.23 seconds** on average for discovering DAEs

Simulation Experiment – Case II

Case I: Milling with time delayed effect, process damping and edge force

Time series trajectories and phase plane plots

- The stability lobe diagram is not presented due to no available methods to obtain the stability solutions of nonlinear governing equations.
- Figure of time domain displacement and Poincare map for exact governing equations and discovered DAEs under noise $r = 1\%$ in Table 4 show the good agreement with each other.

Simulation of discovered governing equations match well with the ground truth → high accuracy of CMML discovered DAEs

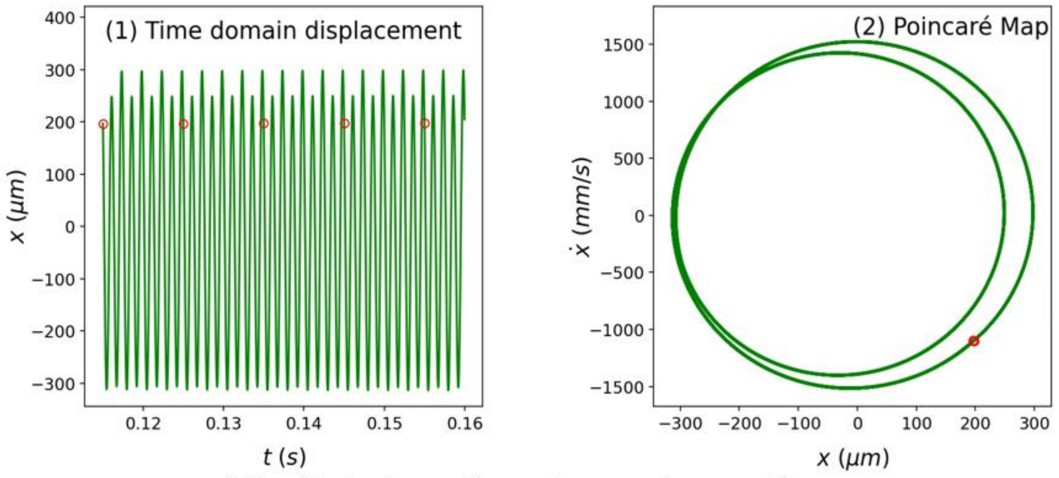

(a) Trajectory of exact governing equations

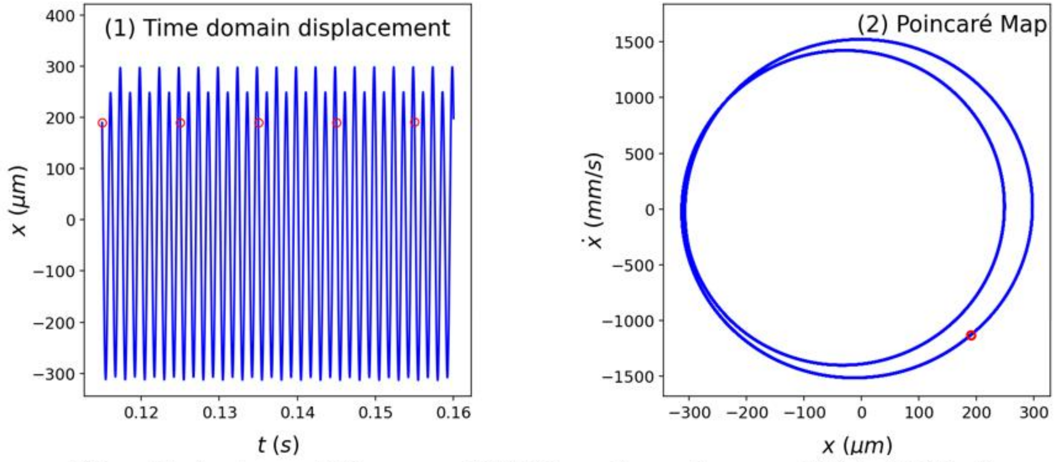

(b) Trajectory of discovered DAEs under noise $r = 1\%$ in Table 4

Time domain displacement (on x direction) and Poincaré map of discovered equations in Table 4 using parameters $\Omega = 6000$ rpm and $b = 2$ mm.

Conclusion and Future Work

Conclusion

- **Conclusion**
  - A cutting mechanics-based machine learning (CMML) modeling method by integrating existing physics in cutting mechanics and unknown physics in data to discover governing equations of machining dynamics.
    - General cutting mechanics-based modeling structure by a set of unknown differential algebraic equations.
    - Discrete optimization-based machine learning to discover the unknown differential algebraic equations.
  - Numerical results show CMML can discover the exact milling dynamics governing equations with time delayed effect, process damping, and edge force from noisy data

- **Next steps**
  - Build effective metrology systems to simultaneously measure the cutting force and at least one among the displacement, velocity and acceleration.
  - Use CMML to discover new experimentally verified cutting force model.

Thank you!

Mason Ma
hma19@vols.utk.edu